LAB-ON-CHIP FOR DNA CONCENTRATION AND SEPARATION WITH A RESOLUTION LENGTH OF 6 BP

Bayan Chami, Marius Socol, Aurélien Bancaud

▶ **To cite this version:**

Bayan Chami, Marius Socol, Aurélien Bancaud. LAB-ON-CHIP FOR DNA CONCENTRATION AND SEPARATION WITH A RESOLUTION LENGTH OF 6 BP. 3rd Conference on MicroFluidic Handling Systems, Oct 2017, Enschede, Netherlands. 4p. hal-01686194

HAL Id: hal-01686194
https://hal.science/hal-01686194

Submitted on 17 Jan 2018

HAL is a multi-disciplinary open access archive for the deposit and dissemination of scientific research documents, whether they are published or not. The documents may come from teaching and research institutions in France or abroad, or from public or private research centers.

L'archive ouverte pluridisciplinaire **HAL**, est destinée au dépôt et à la diffusion de documents scientifiques de niveau recherche, publiés ou non, émanant des établissements d'enseignement et de recherche français ou étrangers, des laboratoires publics ou privés.

LAB-ON-CHIP FOR DNA CONCENTRATION AND SEPARATION WITH A RESOLUTION LENGTH OF 6 BP

B. Chami[1], M. Socol[1] and A. Bancaud[1]
[1] LAAS-CNRS, Toulouse, France

ABSTRACT

DNA separation and analysis has advanced over the last years benefiting from microfluidic systems that reduce sample volumes and analysis cost. We recently developed a microfluidic device that separates and analyzes nucleic acids using bidirectional actuation with a hydrodynamic flow and a counter electrophoretic force in viscoelastic polymer solutions. In this paper, we provide an analytical model of DNA transport by combining hydrodynamics and statistical mechanics capable of predicting the device performances as a function of the experimental control parameters; namely the pressure, the voltage and the fluid rheological properties. The model proves to be in quantitative agreement with the experiments. We finally define conditions for optimal DNA separation in terms of microchannel geometry, fluid viscoelastic properties and electro-hydrodynamic actuation that result in a resolution length (RSL) down to 6 bp.

KEYWORDS

DNA separation, viscoelasticity, resolution, resolution length (RSL).

INTRODUCTION

Transport in viscoelastic flow is gaining interest for particle and cell separation in continuous flow. Viscoelastic fluids have been exploited in the laminar regime or with inertial flows, depending on the throughput requirement of the experiment.

DNA molecules have also been conveyed in viscoelastic flows, showing similar behaviors to nano-objects. We recently showed that the application of a counter electric field offered a solution for high performance size separations as well as enrichment for channels with a funnel geometry [1]. So far, this technology has been applied to the separation of molecules in the size range 200-10000 bp, and we reasoned that its operation principle could be improved for low MW molecules.

Here we provide a quantitative model of DNA transport by combining hydrodynamics, finite-element methods, and statistical mechanics. We observe a very good agreement between our data and the model. One of the purposes of our study is to develop the µLAS device to be able to analyze low molecular weight DNA. This development follows three different roots; development of the channel design, working on the rheological properties of the viscoelastic fluid, and playing with the actuation parameters.

MATERIALS AND METHODS

The design of the microfluidic chips, which are processed by silicon/glass manufacturing[2], consists of a single straight channel with a funnel, as shown in Fig. 1. We define *x* as the longitudinal axis along the flow direction, *y* is along the channel width, and *z* the channel height. The width of the channel is then defined as $A_m x^m$ with *m* the power law of the constriction. The viscoelastic liquid flows in the chip by means of a pressure controller operating in the range 1-10 bar in either direction of the constriction. The electric field is generated using a DC voltage supply operating in the range 0-400 V. Image processing of fluorescence micrographs allows us to monitor the position of the DNA bands of a reference ladder (inset of Fig. 1). The position of the DNA bands is measured using the apex of the constriction as reference.

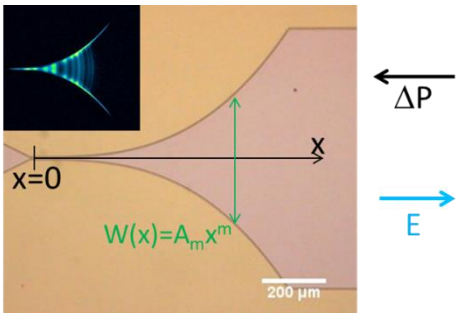

Figure 1: Bright field micrograph of a microchannel with a power-law profile (x^3-profile). The pressure and electric fields are actuated simultaneously in the same direction, but the negative charge of DNA induces an electrophoretic mobility in the opposite direction to the pressure flow. The inset represents a typical image of a DNA molecular weight ladder observed by fluorescence microscopy in the constriction. Each band is assigned to an accumulation position denoted x_{DNA}.

Various concentrations of the viscoelastic fluids used (PVP 1.3 MDa, PVP 40 KDa and PEG 10 KDa), are characterized using particle tracking microrheology[3] and are tested for the separation in different geometries and under several pressure and voltage conditions to determine the fluid resulting in the highest separation performance.

THE PHYSICAL MODEL

Our goal is to express the resolution of DNA separation experiments as a function of the electric

and hydrodynamic actuation parameters and of the fluid viscoelastic properties. For this, we first derive an analytical expression of the transverse viscoelastic force for spherical tracers, and then validate its relevance with finite element simulations. Further, we use statistical physics to infer the distribution of tracers across the channel height, and come up with expressions that predicts the position, width and resolution of a DNA band. These predictions are compared to our experimental results.

Analytical calculation of the transverse viscoelastic force

Let us consider a particle of radius a conveyed by a Poiseuille viscoelastic flow of maximum speed V_{max} in a slit-like channel of height h (Fig. 2A). The shearing leads to an excess of elastic stress that results in transverse migration toward the channel centerline[4]–[6]. For a purely viscoelastic Maxwell fluid, the transverse force F_T reads:

$$F_T(\varepsilon) = -K \times 2\eta\tau \times \pi a^2 \times a \frac{\partial \dot{\gamma}(\varepsilon)^2}{\partial z} \qquad (1)$$

with $\dot{\gamma}$ the shear rate, η the viscosity, τ the fluid relaxation time, and ε the position of the particle. Note that according to the calculations of [5] the proportionality factor K is lower than one and greater than the Reynolds number, which is typically 10^{-4} in our experimental settings.

Considering the contribution of an electrophoretic velocity V_e oriented opposite to the hydrostatic flow and neglecting hydrodynamic interactions and finite-size effects, the velocity of the bead is $V_p(\varepsilon) - V_e$ with $V_p(\varepsilon)$ the hydrodynamic velocity at ε (Fig.2A). The transverse force becomes:

$$F_T^{el}(\varepsilon) = -32K \times \eta\tau\pi a \times \frac{V_p V_e}{h}\left\{1 - \frac{\varepsilon}{h/2}\right\} \qquad (2)$$

This equation applies for particles small compared to the channel height and neglecting pure hydrodynamic components.

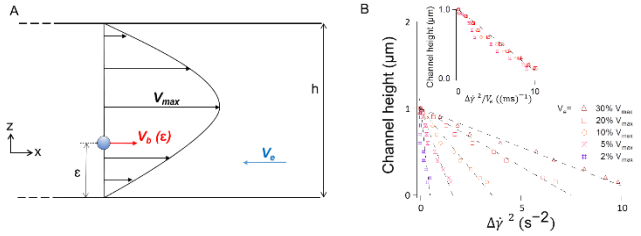

Figure 2: (A) Sketch of a bead at a vertical position ε in a slit-channel of height h. The Poiseuille flow is characterized by its maximum velocity V_{max} and the electrophoretic velocity is V_e. The velocity of the particle is V_b. (B) Using 3D finite element modeling, we measure the difference in square of the shear rate on the upper and lower apex of the particle. The channel height h is set to 2 µm, the particle radius a to 50 nm, the hydrodynamic maximum speed V_{max} to 75 µm/s and different electrophoretic speeds are modeled, as indicated in the inset. The set of data can be rescaled with the electrophoretic velocity (inset).

Validation with finite element simulations

Using 3D finite-element simulations performed with COMSOL, we checked the validity of Eq. (2) for a 100 nm particle flowing in a 2 µm-thick channel. We assumed the fluid to be Newtonian and set the maximum fluid velocity V_{max} to 75 µm/s. We used different electrophoretic velocities spanning 1.5 to 25 µm/s (Fig. 2B). In each condition, the particle was placed at different vertical positions, and we computed the difference between the square of the shear rate on the upper and lower apex of the particle. According to Eq. (2), we expect this data to scale linearly with the particle position and with the electrophoretic velocity. The prediction was quantitatively confirmed because the five simulation datasets could be rescaled with the electrophoretic velocity (inset of Fig. 2B).

Force close to the wall

Close to the walls, i.e. for distances $\varepsilon < 3a$, our analytical model is expected to be invalid as the gradient of flow velocity in between the wall and the particle is unknown. We noted that the COMSOL simulations indicated a reduction of the difference in square of the shear rate for distances in the range 50 to 150 nm (not shown). This result was qualitatively in agreement with the fact that the transverse viscoelastic force should drop to zero at the wall to insure zero-flux conditions. As a first order approximation, we assume that the force linearly drops to zero at the contact. The expression of the force near the wall then reads:

$$F_{T_{wall}}^{el}(\varepsilon) \sim -32K' \times \eta\tau\pi a \times \frac{V_{max} V_e}{h} \times \varepsilon \qquad (3)$$

with K' a dimensional constant equal to K/l with l the difference of slope in Eq. (2). This response is therefore analogous to an elastic spring retaining the sphere at the wall. We can then use Boltzmann statistics to extract the position and distribution of tracers at the wall as a function of the electrophoretic and hydrodynamic velocities.

Prediction for the position, width, and resolution of µLAS

Applying our analytical model, we can deduce the position of a DNA accumulation band, its width, and its separation resolution as shown by Eq. 4, Eq.5 and Eq.6, respectively.

$$x_{DNA}{}^{2m} = K' \times \frac{\eta\tau\pi^2 a h w_0^2}{k_B T A_m{}^2} \times \frac{V_{e,0}{}^3}{V_{max,0}} \quad (4)$$

with w_0 the width of the channel at the apex, and $V_{max,0}$ and $V_{e,0}$ the maximum hydrodynamic and electrophoretic velocities at the apex.

$$B \sim \frac{3\,(\pi-2)^2}{8} K' \sqrt{\frac{\eta a h^3}{k_B T \tau}} \left(\frac{V_{e,0}}{V_{max,0}}\right)^{3/2} \quad (5)$$

Finally, with the definition of the position of the bands and their breadth, it is possible to compute the resolution, as defined as:

$$\frac{Res_{1,2}}{\Delta a_{1,2}} \sim \frac{1}{2m * B_1} a_1^{\left(\frac{1}{2m}-1\right)} \times \left[\frac{K' \eta\tau\pi^2 h w_0^2}{k_B T A_m{}^2} \cdot \frac{V_{e,0}{}^3}{V_{max,0}}\right]^{\frac{1}{2m}} \quad (6)$$

where $\Delta a_{1,2}$ the difference in size between two consecutive DNA bands. Note that we could also express the breadth B_1 using Eq. (5), but this additional calculation does not improve the fitting of our data. The right term in Equation (6) is the inverse of the resolution length (RSL) [7], which defines the minimal genomic distance between two consecutive peaks that can be separated with the technology.

RESULTS

Separation of 50-1000 bp DNA bands

By comparing the separation of a 50 bp DNA ladder in a linear versus a power-law geometry using the same viscoelastic solution PVP (40 KDa, 18% (wt%)) and under the same actuation parameters P-V (7 bar-300 V); at least a 25 bp RSL separation is possible with the power-law profile and not with the linear profile (Fig.4). The intensity profiles shown in Fig.4 (B) and (D) clearly show that the power-law profile allows the separation of DNA molecular weight lower than 200 bp.

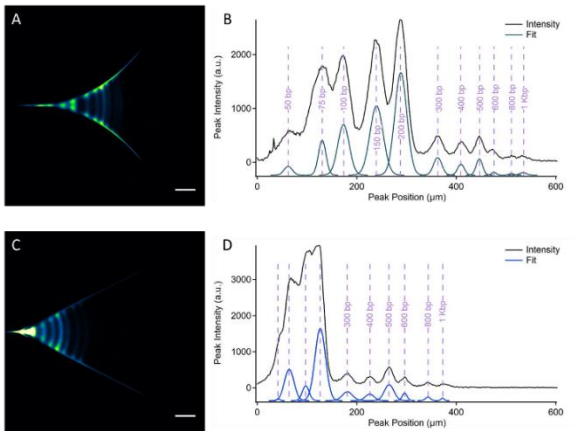

Figure 3: (A) and (C) The fluorescence images of a 50 bp DNA ladder separated in the power law profile and the linear profile, respectively (scale bar 100 µm). (B) and (D) The detected fluorescence intensity profiles of the DNA bands corresponding to (A) and (C), respectively.

Now that the power-law geometry has proved to be better than the linear one for separating low MW DNA, we use it to compare different polymer solutions. The rheological properties of all the tested solutions obtained using microrheology are displayed in Table 1.

Table 1: Viscosity (mPa.s) and Elasticity (Pa) of tested polymer solutions.

(MW)	(wt%)	Viscosity η (mPa.s)	Elasticity E (Pa)
PVP 40 KDa	10	6 ± 1.2	0.40 ± 0.07
	13	8 ± 1.3	0.50 ± 0.08
	15	9.5 ± 1.3	0.67 ± 0.13
	18	12 ± 1.25	0.85 ± 0.1
	20	14.5 ± 1.2	0.95 ± 0.3
PEG 10 KDa	20	12.7 ± 1.1	1.34 ± 0.3
PVP 1.3 MDa	2	6 ± 0.4	0.33 ± 0.08
	3	8 ± 1.3	0.45 ± 0.1
	4	19 ± 2	0.61 ± 0.1
	5	23 ± 1.25	0.50 ± 0.12

After testing all the viscoelastic fluids presented in Table 1 and choosing those that result in the best separations, the RSL obtained by each was calculated for all the DNA bands of the ladder and shown in Fig.4.

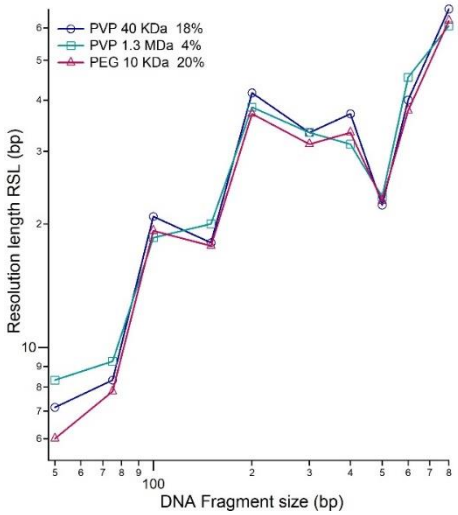

Figure 4: RSL for different polymer solutions at the optimal conditions of each.

From Fig.4 and the table, it can be concluded that the viscosity and the elasticity of the polymer solution play an important role in determining the separation performance of the device.

Validation of the physical model

The position and width of a DNA band

The data obtained from several experiments prove to fit the model perfectly as shown in Fig. 5 (A-D).

The slopes of the different fits change with the polymer solution showing a dependence on the rheological properties of the viscoelastic fluids as predicted by our model.

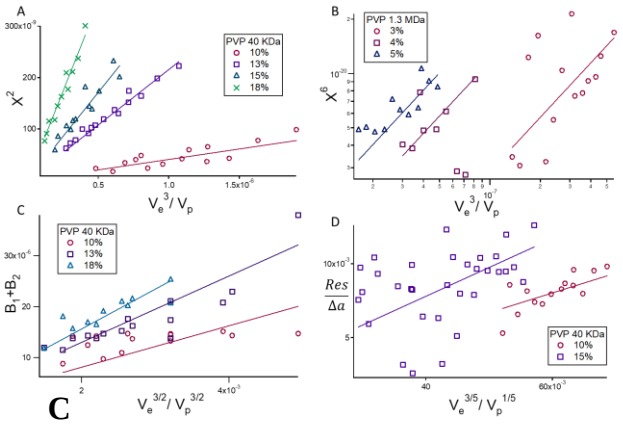

C

Figure 5: Model-Data fit. (A) The position of a 600 bp DNA band in a linaer geometry (m=1) for different concentrations of PVP 40 KDa. (B) The position of a 300 bp band in a power-law geometry (m=3) for different concentrations of PVP 1.3MDa. (C) The width of a 600 bp DNA band in a in a power-law geometry (m=2.5) in PVP 40 KDa at different concentrations. The inverse RSL of a 600 bp band in the power-law geometry (m=2.5) in PVP 40 KDa (10% and 15%).

CONCLUSION

The improvement of a new DNA separation and analysis technology, based on bidirectional electro-hydrodynamic actuation in viscoelastic fluids, was carried out through optimization of the microfluidic chip design and the viscoelastic fluid rheological properties. A physical model based on hydrodynamics and statistical mechanics and validated by finite element simulations enabled us to predict the device performance. A power-law chip design proved to be better than a linear design for the separation of DNA fragments smaller than 200 bp and a RSL of at least 25 bp was reached. Further improvement involving the viscoelastic fluid resulted in a RSL of 6 bp. Finally, the physical model fit the experimental data and provided insights for further developments.

REFERENCES

[1] H. Ranchon *et al.*, "DNA separation and enrichment using electro-hydrodynamic bidirectional flows in viscoelastic liquids," *Lab Chip*, vol. 16, no. 7, pp. 1243–1253, 2016.

[2] B. M. Paegel, R. G. Blazej, and R. A. Mathies, "Microfluidic devices for DNA sequencing: sample preparation and electrophoretic analysis," *Curr. Opin. Biotechnol.*, vol. 14, no. 1, pp. 42–50, Feb. 2003.

[3] T. G. Mason, K. Ganesan, J. H. van Zanten, D. Wirtz, and S. C. Kuo, "Particle Tracking Microrheology of Complex Fluids," *Phys. Rev. Lett.*, vol. 79, no. 17, pp. 3282–3285, Oct. 1997.

[4] G. D'Avino, F. Greco, and P. L. Maffettone, "Particle Migration due to Viscoelasticity of the Suspending Liquid and Its Relevance in Microfluidic Devices," *Annu. Rev. Fluid Mech.*, vol. 49, no. 1, pp. 341–360, Jan. 2017.

[5] B. P. Ho and L. G. Leal, "Migration of rigid spheres in a two-dimensional unidirectional shear flow of a second-order fluid," *J. Fluid Mech.*, vol. 76, no. 04, p. 783, Aug. 1976.

[6] A. M. Leshansky, A. Bransky, N. Korin, and U. Dinnar, "Tunable Nonlinear Viscoelastic 'Focusing' in a Microfluidic Device," *Phys. Rev. Lett.*, vol. 98, no. 23, Jun. 2007.

[7] Y. Yamaguchi, Z. Li, X. Zhu, C. Liu, D. Zhang, and X. Dou, "Polyethylene Oxide (PEO) and Polyethylene Glycol (PEG) Polymer Sieving Matrix for RNA Capillary Electrophoresis," *PLOS ONE*, vol. 10, no. 5, p. e0123406, May 2015.